

A Cryosolution Infrared Study of the Complexes of Fluoroform with Ammonia and Pyridine: Evidence for a C–H···N Pseudo Blue-Shifting Hydrogen Bond

Wouter A. Herrebout,[†] Sonia M. Melikova,[‡] Sofie N. Delanoye,[†] Konstantin S. Rutkowski,[‡] Dimitri N. Shchepkin,[‡] and Benjamin J. van der Veken^{*,†}

Department of Chemistry, University of Antwerp, Groenenborgerlaan 171, B-2020, Antwerp, Belgium, and Institute of Physics, St. Petersburg University, Ulianovskaia 1, 198504, Peterhof, St. Petersburg, Russia

Received: November 9, 2004; In Final Form: February 9, 2005

Mid-infrared spectra of mixed solutions in liquid xenon containing fluoroform and either ammonia or pyridine have been investigated at temperatures between 173 and 213 K. For both Lewis bases, a new band is found in the CH stretching region at a frequency approximately 5 cm⁻¹ higher than that of monomer fluoroform, which is assigned to a complex between fluoroform and the Lewis base. A detailed analysis of the $\nu_1/2\nu_4$ Fermi resonance in the proton donor shows that the blue shifts observed for the complexes are not caused by a strengthening of the CH bond during the complexation, but are due to the changes in the Fermi resonance interactions. Information on the $\nu_1/2\nu_4$ Fermi resonance was also obtained for the complexes of fluoroform with dimethyl ether and trimethyl amine.

Introduction

In theoretical as well as in experimental studies, fluoroform, CHF₃ (Fl), is a popular Lewis acid in investigations of the weak hydrogen bonds formed by C–H bonds.^{1–24} It owes its popularity to the fact that upon the formation of a hydrogen bond, the C–H bond can either be weakened, that is, lengthened, which is the more traditional pattern, or it can be strengthened, that is, shortened. In the former case the C–H stretching mode $\nu_1(A_1)$ is expected to red-shift from its position in the monomer; in the latter case, described as improper or blue-shifting hydrogen bonding,^{7,12,14,19,21} it should give rise to a blue shift.

For Fl, predictions on the type of hydrogen bonding based on the observed shift of ν_1 are complicated by the fact that the first excited level of that mode is in Fermi resonance with the A₁ component of the first overtone level $2\nu_4$ of the degenerate C–H bending mode $\nu_4(E)$. It is known from previous studies that ν_4 of fluoroform is very sensitive to the formation of a complex, with the mode in general shifting to higher frequency, by an amount depending on the strength of the complex.^{15,16} This implies that there is a considerable complexation shift on $2\nu_4$, which, combined with the change in the C–H bond strength, most likely will change the resonance condition. When this occurs, the observed shift for ν_1 is the sum of two contributions, a shift induced by the complexation and a shift caused by the change in the Fermi resonance. As these may have opposite signs, it follows that the observed shift no longer is a measure for the change in the C–H bond strength.

In this study we report on the infrared spectra of the 1:1 hydrogen bonded complexes of Fl with ammonia, NH₃ (Am), pyridine, C₅H₅N (Py), dimethyl ether, (CH₃)₂O (DME), and trimethyl amine, (CH₃)₃N (TMA), as they are formed in cryosolutions, using liquid argon (LAr) or liquid xenon (LXe) as a solvent. It will be demonstrated that the ν_1 of Fl in the complexes with Am and Py is detected slightly blue shifted from

its position in the monomer. In view of what is said in the previous paragraph, it is clear that this observation does not suffice to categorize the hydrogen bonding in these complexes as improper. To be able to identify the bonding type, we report on the correction of the observed ν_1 frequencies for the Fermi resonance, and we will show that at least for the complex with pyridine the bonding type is in fact of the traditional, red-shifting type.

The complexes of Fl with DME^{9,24} and TMA² have been studied before in LAr, however, without considering the Fermi resonance problem. In this study we aim at showing that also for these complexes the corrections for Fermi resonance are significant, but that they do not lead to conclusions on the hydrogen bonding type different from the ones previously proposed.

Experimental and Computational Details

The samples of Py-d₅, Am, DME-d₆, TMA-d₉ were obtained from Aldrich and Fl was provided by Praxair. The solvent gases used were obtained from Air Liquide and had stated purities of 99.9999% (Ar) and 99.995% (Xe). The solvent gases and the chemicals were used without further purification.

The infrared spectra were recorded on a Bruker IFS 66v Fourier transform spectrometer, using a Globar source in combination with a Ge/KBr beam splitter and a broadband MCT detector. In general, the interferograms were averaged over 300 scans, Happ Genzel apodized, and Fourier transformed using a zero-filling factor of 4 to yield spectra at a resolution of 0.5 cm⁻¹.

A detailed description of the liquid noble gas setup was given previously.¹¹ Liquid cells with path lengths of 1 and 7 cm, equipped with wedged silicon and wedged ZnSe windows, respectively, were used to record the spectra.

Geometries and vibrational frequencies of the 1:1 complexes were obtained from ab initio and DFT calculations, at various levels of at least 6-31+G(d,p) quality. During the geometry optimizations and the force field calculations, corrections for

* Corresponding author. E-mail: benjamin.vanderveken @ua.ac.be.

[†] University of Antwerp.

[‡] St. Petersburg University.

TABLE 1: Calculated Properties for Fluoroform and for Its Complexes with Ammonia, Pyridine, Dimethyl Ether, and Trimethyl Amine^a

	Fl•Am		Fl•Py	Fl•DME	Fl•TMA
	MP2/6-311++G(3df,2pd)	MP2/6-31+G(d,p)	MP2/6-31+G(d,p)	MP2/6-31+G(d,p)	MP2/6-31+G(d,p)
$\Delta E/\text{kJ mol}^{-1}$	-16.5	-18.5	-19.5	-17.4	-19.4
$r_{\text{X}\cdots\text{H}}/\text{\AA}$	2.367	2.370	2.336	2.217	2.295
$\Delta r_{\text{CH}}/10^{-3} \text{\AA}$	0.6	1.0	0.5	-0.7	3.6
$\nu_1(\text{monomer})/\text{cm}^{-1}$	3200.0	3270.3	3270.3	3270.3	3270.3
$\nu_1(\text{complex})/\text{cm}^{-1}$	3193.8	3261.3	3266.7	3287.5	3219.0
$\Delta\nu_1/\text{cm}^{-1}$	-6.2	-9.0	-3.6	+17.2	-51.3
$I_1(\text{monomer})/\text{km mol}^{-1}$	24.4	24.8	24.8	24.8	24.8
$I_1(\text{complex})/I_1(\text{monomer})$	0.39	0.43	0.60	0.20	1.18
$\nu_4(\text{monomer})/\text{cm}^{-1}$	1417.6	1419.9	1419.9	1419.9	1419.9
$\nu_4(\text{complex})/\text{cm}^{-1}$	1457.4	1454.7	1449.6/1447.8	1445.8/1439.7	1466.3
$\Delta\nu_4/\text{cm}^{-1}$	39.8	34.8	29.7/27.9	25.9/19.8	46.4

^a Values obtained using the CP-corrected PES.

BSSE were taken into account explicitly using the CP corrected gradient techniques of Simon et al.²⁵ All calculations were performed using Gaussian03.²⁶ To reduce numerical errors during the analysis, the eigenvectors L_i describing the normal vibrations were obtained using the *Freq=Hpmodes* keyword.

Results and Discussion

A. Theoretical Predictions of the Complexation Shifts.

Some theoretical results are available in the literature for Fl•Am. A very nearly C_{3v} structure with a C–H···N angle of 179.7 degrees was obtained by Schlegel et al.¹⁴ at the MP2=FC/6-311+G(d,p) level. These calculations predict a complexation red shift by -0.8 cm^{-1} for ν_1 of the Fl moiety. DFT calculations at the 6-311++G(3df,2pd) level predict a much larger red shift of -13 cm^{-1} for the same mode.¹⁶ Recently, MP2 calculations at the 6-311G(d), 6-311+G(d,p), and aug-cc-PVDZ levels have been shown to predict red shifts of -8 , -2 , and -13 cm^{-1} , respectively.²³

The 255 function basis set 6-311++G(3df,2pd) is the largest used for Fl•Am up to now. However, there are some doubts about the way the applied DFT method accounts for dispersion interactions, which for weak complexes of the present type are known to be relatively significant. Therefore, we have expanded the available data on Fl•Am with MP2 calculations at that level. The complex is found to have C_{3v} symmetry. Data relevant to the present study have been collected in Table 1. It can be seen that, in a direction consistent with published data, a red shift is predicted for ν_1 , by -6.2 cm^{-1} , which falls within the interval of the published values.

Apart from the above results for Fl•Am, Table 1 contains MP2/6-31+G(d,p) data for all complexes studied here. The smaller basis set was adopted to reduce the computational effort for the larger complexes. We justify its use by the following facts. For Fl•Am the smaller basis set predicts a shift for ν_1 in the same direction as the larger basis set, albeit that the quantitative agreement is not optimal. Also, calculations using the 6-31++G(d,p) basis set, i.e., a basis set containing diffuse functions for the hydrogen atoms, result in complexation shifts of ν_1 differing by not more than 3.7% (trimethyl amine), 0.6% (pyridine), and 3% (dimethyl ether). This consistency in the direction of the ν_1 shifts then allows the suggestion that at least the directions of the ab initio shifts in Table 1 are reliable.

For Fl•TMA and Fl•Am the calculations lead to C_{3v} symmetry, and for Fl•Py and Fl•DME to C_s symmetry. It follows from Table 1 that the hydrogen bonding in complexes with Am, Py and TMA is predicted to be of the traditional type, while, in agreement with experiment,^{9,24} for the DME complex a blue-shifting hydrogen bond is present.

The results in Table 1 confirm the high complexation sensitivity of ν_4 of Fl. Taking the average values for the C_s complexes, the predicted shifts vary by more than a factor of 2, from 22.9 cm^{-1} for Fl•DME to 46.4 cm^{-1} for Fl•TMA. At the same time, the complexation energies vary in a much narrower interval, between -17.4 and $-19.5 \text{ kJ mol}^{-1}$. Inspection of Table 1 shows that, in disagreement with previous conclusions,^{15,16} the correlation of the ν_4 shifts with the complexation energies is not very strong, as the shift for Fl•Am exceeds that of Fl•Py, while the former has the lower complexation energy.

B. Vibrational Spectra. Solubilities of Fl, DME, and TMA in liquid argon are such that the complexes Fl•DME and Fl•TMA can be studied in that solvent. The solubilities of Am and Py are very low in liquid argon and in liquid krypton, so these complexes had to be investigated in liquid xenon. Relevant observed frequencies have been collected in Table 2. Comparison with Table 1 shows that the experimental and calculated complexation shifts of ν_1 are in the same direction for the complexes with DME and TMA, while for the Py and Am complexes they are in opposite directions.

In Figure 1 the spectrum of the ν_1 region of monomer Fl is compared with those of Fl•Am and Fl•Py in panel A and with those of Fl•DME and Fl•TMA in panel B. In all cases the spectrum of the complex was isolated by subtracting out the monomer contributions. The sharper features in Figure 1A at 3038.1 in Fl•Am and at 3033.3 cm^{-1} in Fl•Py are slightly blue shifted, by 7.6 and 3 cm^{-1} , respectively, from the ν_1 band in monomer Fl and are assigned to that mode in the complexes. For Fl•Am the blue shift is remarkable because in a matrix isolation study in solid argon this mode was detected red shifted by -21 cm^{-1} .⁴ We will return to this point in a later paragraph.

Figure 1B shows that ν_1 is red shifted, by -23 cm^{-1} , in Fl•TMA but blue shifted, by 18 cm^{-1} , in Fl•DME. The sharp, weak band at 2700.2 cm^{-1} in the spectrum of monomer Fl in LXe is assigned as $2\nu_4^A$. It can be seen that for both complexes the changes in this transition are similar to those observed for the complexes in Figure 1A. In the complexes, these transitions can be seen to have considerably higher relative intensity and to be substantially blue shifted. The band areas, which we identify with the integrated intensities, of ν_1 and $2\nu_4^A$ have been determined, for Fl and for the complexes, using numerical integration. The ratio of the integrated intensities $R = I(\nu_1)/I(2\nu_4^A)$ is 28(5) and 36(5) for monomer Fl in LAr and LXe, respectively, but decreases to values between 2.6(3) and 1.5(2) for the complexes (see Table 2). From an a priori point of view, several reasons for such a dramatic decrease in relative intensity could be suggested. We believe, for the reasons explained in

TABLE 2: Spectroscopic Parameters for Fluoroform and for Its Complexes with Dimethyl Ether, Trimethyl Amine, Ammonia, and Pyridine

	LAr, 90 K			LXe, 188 K		
	FI	FI·DME	FI·TMA	FI	FI·Am	FI·Py
ν_4/cm^{-1}	1374.5(2)	1390.2(5)	1405.9(5)	1372(1)	1391.4(5)	1388.8(5)
ν_1/cm^{-1}	3036.7(2)	3054.8(2)	3013.9(3)	3030.5(3)	3038.1(5)	3033.3(5)
$\Delta\nu_1/\text{cm}^{-1}$		18.1	-22.8		7.6	3
$2\nu_4/\text{cm}^{-1}$	2704.7(5)	2737(1)	2749(1)	2700.2(5)	2741(1)	2739(2)
ν_1^0/cm^{-1}	2990.2(3)	3005.3(3)	2946.7(5)	2983.6(3)	2983.3(5)	2977.6(5)
$\Delta\nu_1^0/\text{cm}^{-1}$		+15.1(4)	-43.5(6)		-0.3(6)	-6.0(6)
$\Sigma/\text{km mol}^{-1}$	20(2)	4.4(5)	17(3)	23(2)	9.8(1)	10(2)
$R(\text{expt})$	28(5)	1.5(2)	1.5(2)	36(5)	2.3(3)	2.6(3)
$R(\text{calc})$	14	1.9	2.2	12.6	2.2	2.2
$\langle 00 \mu_z 10\rangle_{\text{exp/D}}$	-0.052	0.024	0.048	-0.055	0.036	0.036
$\langle 00 \mu_z 10\rangle_{\text{cal/D}}$	-0.055 ^a	0.025 ^a	0.060 ^a	-0.055 ^a	0.036 ^a	0.043 ^a
					0.049 ^b	0.075 ^b

^a Derived from MP2/6-31+G(d,p) calculations. ^b Taken from ref 15 from DFT B3LYP/6-311++G(3df,3pd) calculations.

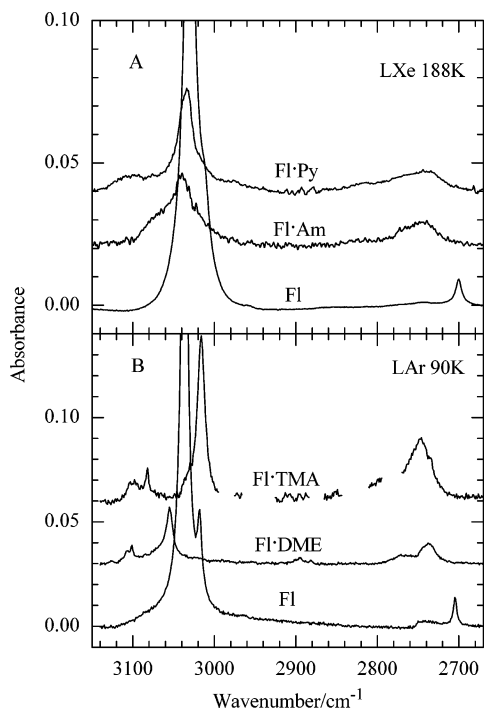


Figure 1. Comparison of the fluoroproform ν_1 region observed for monomer fluoroproform and its complexes with ammonia, pyridine, dimethyl ether, and trimethyl amine. The spectra of FI·Am and FI·Py (A) were recorded using LXe as a solvent. The spectra of FI·DME and FI·TMA (B) were recorded using LAr as a solvent.

the next paragraph, that it is due to the complexation influence on the parameters of the Fermi resonance between ν_1 and $2\nu_4^{A_1}$.

An evident origin for a change in the Fermi parameters would be a shift of the unperturbed overtone level $(2\nu_4^{A_1})^0$, which must be related to the complexation behavior of the fundamental ν_4 . Therefore, in Figure 2 the region of ν_4 of the monomer and of the complexes is given. It can be seen that in all cases the complexation induces an upward shift in ν_4 . Although the correlation of the experimental $\Delta\nu_4$'s with the predicted values in Table 1 is not very high, both series can be seen to increase in the same order, with the experimental values systematically smaller. This shift causes a blue shift of $2\nu_4^{A_1}$, with an ensuing change in the resonance condition.

The sum of absolute intensities $\Sigma = I(\nu_1) + I(2\nu_4^{A_1})$ was evaluated from the observed ratio $\Sigma/I(\nu_6)$ and by using literature data on the infrared intensity $I(\nu_6) = 4.8 \text{ km/mol}^{27}$. The ν_6 band, assigned as a CF-bending vibration, is not significantly affected upon complexation. This assumption is supported by a wide

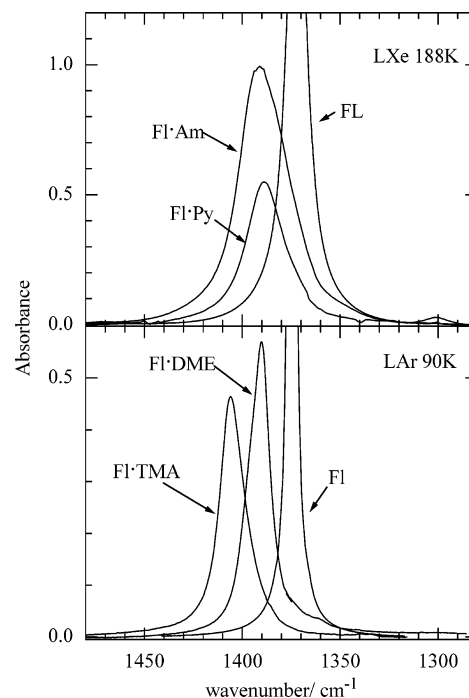


Figure 2. Comparison of the fluoroproform ν_4 region observed for monomer fluoroproform and its complexes with ammonia, pyridine, dimethyl ether, and trimethyl amine. The spectra of FI·Am and FI·Py (A) were recorded using LXe as a solvent. The spectra of FI·DME and FI·TMA (B) were recorded using LAr as a solvent.

set of DFT and MP2 calculations^{15,16} and is confirmed by our MP2 calculations on FI·Am ($I(\nu_6)^{\text{mono}} = 6.4 \text{ km/mol}$ and $I(\nu_6)^{\text{comp}} = 6.8 \text{ km/mol}$). The resulting values of Σ are given in Table 2. The quantity Σ is invariant under the Fermi resonance, from which follows that it must be equal to the sum of the intensities of the unperturbed transitions:

$$\Sigma = I(\nu_1) + I(2\nu_4^{A_1}) = I(\nu_1)^0 + I(2\nu_4^{A_1})^0 \quad (1)$$

where

$$I(\nu_1)^0 = \frac{8\pi^3 N_A \nu_1 10^{-13}}{3hc} \langle 00^0 | \mu_z | 10^0 \rangle^2$$

$$I(2\nu_4^{A_1})^0 = \frac{8\pi^3 N_A \nu_1 10^{-13}}{3hc} \langle 00^0 | \mu_z | 02^0 \rangle^2 \quad (2)$$

where the ν_i are the transition frequencies ν_1 and $2\nu_4$, respectively.

The unperturbed second-order transition dipole ($\langle 00^0 | \mu_z | 02^0 \rangle^0$) was evaluated from an ab initio grid calculation (see eq 6 and Table 4) and was found to equal 0.006 D both for FI and for the complex FI·Am. From this quantity one obtains $I(2\nu_4^A)^0 = 0.2$ km/mol. The values of $\langle 00^0 | \mu_z | 10^0 \rangle_{\text{exp}}^0$ in Table 2 were derived from the quantities $I(\nu_1)^0 = \Sigma - 0.2$ km/mol for all the systems studied. The sign of the transition moment cannot be derived from the intensities and, therefore, was taken from ab initio calculations at the MP2/6-31+G(d,p) level. The transition dipoles obtained in this way are compared with the ab initio values in the bottom two rows of Table 2.

C. Fermi Resonance. To correct the observed ν_1 frequencies for Fermi resonance, the implications for the two different symmetries must be considered. For the compounds with C_{3v} symmetry the unperturbed fundamental level ν_1^0 is coupled to the overtone level $2\nu_4^A \equiv 2\nu_4^0$ via the coupling matrix element $W = -\alpha_{144}/\sqrt{2}$, in which α_{144} is a cubic anharmonicity constant. For the complexes with C_s symmetry the two-fold degeneracy of ν_4 is lifted, resulting in levels ν_{4a} and ν_{4b} . In this case ν_1^0 is coupled to $2\nu_{4a}^0$ via $\alpha_{14a4a}/2$, and to $2\nu_{4b}^0$ via $\alpha_{14b4b}/2$, while $2\nu_{4a}^0$ and $2\nu_{4b}^0$ are coupled via the quartic force constant $\beta_{4a4a4b4b}$. The corresponding terms in the potential energy expansion in dimensionless normal coordinates are

$$\alpha_{144}Q_1(X_4^2 + Y_4^2) + \beta_{4444}(X_4^2 + Y_4^2)^2 \quad (3a)$$

for C_{3v} and

$$\alpha_{14a4a}Q_1X_4^2 + \alpha_{14b4b}Q_1Y_4^2 + \beta_{4a4a4a4a}X_4^4 + 2\beta_{4a4a4b4b}X_4^2Y_4^2 + \beta_{4b4b4b4b}Y_4^4 \quad (3b)$$

for C_s . Here we assume that $\alpha_{14a4b} = \beta_{4a4a4a4b} = \beta_{4a4b4b4b} = 0$. For the C_{3v} molecules X_4 and Y_4 are the polar coordinates describing the degenerate ν_4 couple, the sum of their squares having the correct symmetry. For the C_s complexes these coordinates evidently describe the two nondegenerate components that arise from the lifting of the degeneracy.

Given a value for α_{144} , the two-dimensional degenerate case (C_{3v}) is easily solved for the unperturbed levels, as ν_1^0 and $2\nu_4^0$ can be obtained from the unperturbed splitting $\Delta = \nu_1^0 - 2\nu_4^0$, which is calculated from the well-known relation $\Delta = \sqrt{\kappa^2 - 4W^2}$, in which κ is the observed splitting. Treatment in full of the three-dimensional nondegenerate case (C_s) is neatly more complicated. It can be shown (see below), however, that in this case it is also possible to treat the Fermi resonance using the two-dimensional degenerate approximation.

Experimental values for the cubic coupling constant α_{144} in vapor phase monomer FI have been determined to be 100 cm^{-1} ^{28,29} and 170 cm^{-1} .³⁰ The former value was obtained by fitting the tri-diagonal Fermi resonance Hamiltonian of higher-order transitions involving the ν_1 and ν_4 modes, while the latter value was derived assuming that the unperturbed anharmonicity constants x_{44}^0 and g_{44}^0 are zero. Theoretical values of approximately 200 cm^{-1} for this constant have also been reported in the literature.^{31–34} We have calculated α_{144} and quartic anharmonicity constant β_{4444} for monomer FI by MP2 and DFT grid calculations, using basis sets ranging from 6-31+G(d,p) to 6-311++G(2d,2p) level. The obtained values for α_{144} vary between 198.4 and 209.6 cm^{-1} , and those of β_{4444} between 13.9 and 16.7 cm^{-1} . The values of α_{144} confirm previous theoretical values. Using DFT calculations at the B3LYP/6-31++G(d,p) level, we have obtained values for the same constants in the complexes. The results are given in Table 3. They can be seen

TABLE 3: B3LYP/6-31++G(d,p) Cubic and Quartic Force Constants, in cm^{-1} , for Monomer Fluoroform and for Its Complexes with Ammonia, Pyridine, Dimethyl Ether, and Trimethyl Amine

	symmetry	α_{14a4a}	α_{14b4b}	$2\beta_{4a4a4b4b}$
FI	C_{3v}	204.0	204.0	15.1
FI·Am	C_{3v}	200.7	200.7	12.8
FI·Py	C_s	202.0	201.5	13.0
FI·DME	C_s	206.2	204.1	13.5
FI·TMA	C_{3v}	200.2	200.2	10.9

to support the approximation that the complexation influence on α_{144} is sufficiently small to be neglected. This strictly applies only to the isolated molecules, but there is no reason complexation in cryosolution should induce strong changes in either α_{144} or β_{4444} .

At this point, justification of the degenerate approximation used for the Fermi correction in the C_s complexes can be given. By using data from the Tables 1 and 3, model calculations were made in which a three-dimensional matrix for the nondegenerate case was diagonalized. These calculations indicate that the influence on ν_1 of the relatively small values of $\beta_{4a4a4b4b}$ (~ 8 cm^{-1}) is limited. Inversely, the calculations show that for chosen values of ν_1 and α_{144} the degenerate approximation but slightly overestimates the values of ν_1^0 from the nondegenerate approximation by a mere ~ 0.01 cm^{-1} .

All of the above data, both experimental and theoretical, situate α_{144} in the interval between 100 and 200 cm^{-1} . The influence of the value of α_{144} on the unperturbed complexation shift $\Delta\nu_1^0 = \nu_1^0(\text{complex}) - \nu_1^0(\text{monomer})$ in this fairly wide interval has been calculated and is shown in Figure 3. It can be seen that for the weakest complex, FI·DME, the unperturbed complexation shift depends only weakly on the value of α_{144} , $\Delta\nu_1^0$ varying from +17 to +13 cm^{-1} in the interval considered. The same is not true for the strongest complex, FI·TMA, where $\Delta\nu_1^0$ varies from -28 cm^{-1} for $\alpha_{144} = 100$ cm^{-1} to -70 cm^{-1} for $\alpha_{144} = 186$ cm^{-1} , at which value the resonance is exact. The necessity of using the correct value of α_{144} in the deperturbation of the ν_1 frequencies becomes clear from the behavior of the other two complexes: Figure 3 shows that in the interval considered, they both see a switch of their bonding

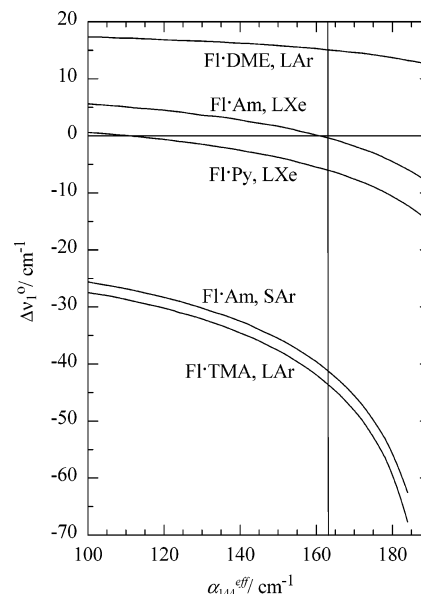


Figure 3. Calculated values for the unperturbed complexation shifts $\Delta\nu_1^0$ as a function of the cubic coupling constant $\alpha_{144}^{\text{eff}}$. The data for FI·Am in a solid argon matrix at 20 K are based upon ref 4.

type from blue- to red-shifting. This occurs at $\alpha_{144} = 110 \text{ cm}^{-1}$ for FL·Py and at $\alpha_{144} = 160 \text{ cm}^{-1}$ for Fl·Am.

We have derived an experimental value of α_{144} for monomer Fl using experimental vapor phase data^{28,29} for 32 transitions involving the ν_1 and ν_4 modes (up to $N = \nu_1 + \nu_4/2 = 6$) and taking into account higher order interactions in the Fermi resonance Hamiltonian. This leads to an effective cubic coupling constant³⁵ $\alpha_{144}^{\text{eff}}$ which depends on the vibrational quantum numbers as:

$$\alpha_{144}^{\text{eff}}(\nu_1, \nu_4) = -\frac{2\sqrt{2}}{(\nu_4 + 2)\sqrt{\nu_1}} \langle \nu_1, \nu_4^0 | V | \nu_1 - 1, (\nu_4 + 2)^0 \rangle$$

which for the present case results in

$$\alpha_{144}^{\text{eff}}(1,0) \equiv \alpha_{144}^{\text{eff}} = \alpha_{144} \left[1 + \frac{3}{2} \nu_1 \gamma_1 + 2(\nu_4 + 2) \gamma_2 \right] \quad (4)$$

where $\alpha_{144} = 182(2) \text{ cm}^{-1}$, $\gamma_1 = -0.035$, $\gamma_2 = -0.016$,³⁵ so $\alpha_{144}^{\text{eff}} = 161(2) \text{ cm}^{-1}$. An analogous result was obtained for Fl in LK_r from 16 observed frequencies: $\alpha_{144}^{\text{eff}} = 163(2) \text{ cm}^{-1}$.

Using the above value of $163(2) \text{ cm}^{-1}$ for $\alpha_{144}^{\text{eff}}$, the unperturbed frequencies ν_1^0 and complexation shifts $\Delta\nu_1^0$ have been calculated. They are given in Table 2. For Fl·DME the Fermi correction yields a $\Delta\nu_1^0$ value that is lower than the observed one. However, the obtained value ascertains beyond doubt that this complex is held together by an improper, blue-shifting hydrogen bond. As could be anticipated from Figure 3, the unperturbed $\Delta\nu_1^0$ for Fl·TMA is considerably larger than the observed value. For Fl·Py the Fermi correction changes the type of the interaction from blue- to red-shifting. For Fl·Am the result is less clear: the significantly blue-shifted value of the unperturbed ν_1 is corrected into a frequency which is a mere 0.3 cm^{-1} below the corrected value for monomer Fl. Although this removes the certainty suggested by the unperturbed value that the bonding is of the blue-shifting type, in the light of the potential sources of uncertainty, the red shift of -0.3 cm^{-1} is too small to ascertain that this complex is of the red-shifting type, the only evidence for the latter being the matrix shift of -21 cm^{-1} .

The other important characteristic of the complexation of Fl is the sharp change in the relative intensity $R = I(\nu_1)/I(2\nu_4^{\text{A}_1})$ of the Fermi doublet, from $R \sim 30$ in the monomer to $R \sim 1$ in the complexes. This change can be rationalized using a first-order perturbation description of the intensities.

In a first step, the Fermi unperturbed transition moments must be established. For the present purpose we retain the zeroth-order approximation for the unperturbed transition dipole of the fundamental, as this is by far the dominant term:

$$\langle 00 | \mu_z | 10 \rangle = \frac{1}{\sqrt{2}} \left(\frac{\partial \mu_z}{\partial Q_1} \right)_e + \dots \quad (5)$$

For the overtone

$$\begin{aligned} \langle \langle 00 | \mu_z | 02^0 \rangle \rangle^0 &= -\frac{1}{2} \left(\frac{\partial^2 \mu_z}{\partial (X_4^2 + Y_4^2)} \right)_e + \\ &\frac{\alpha_{144}}{2(\omega_1 + 2\omega_4)} \left(\frac{\partial \mu_z}{\partial Q_1} \right)_e + \sum_{s=2,3} \frac{\alpha_{s44} \omega_2}{\omega_s^2 - 4\omega_4^2} \left(\frac{\partial \mu_z}{\partial Q_s} \right)_e + \dots \quad (6) \end{aligned}$$

where the ω_i are the harmonic frequencies.

TABLE 4: Cubic Coupling Constant α_{144} , Dipole Moment Derivatives and the Second-Order Transition Moments of Fluoroform and Its Complex with Ammonia Resulting from MP2(Fc)/6-31+G(d,p) Grid Calculations

	Fl	Fl·Am
$\alpha_{144}/\text{cm}^{-1}$	200(5)	203(5)
$\left(\frac{\partial \mu_z}{\partial Q_1} \right)_e / D$	-0.0762(1)	0.0432(2)
$\frac{1}{2} \left(\frac{\partial^2 \mu_z}{\partial (X_4^2 + Y_4^2)} \right)_e / D$	-0.0069(1)	-0.0048(1)
$\langle 02^0 \mu_z 00^0 \rangle / D$	0.0058(2)	0.0056(2)

The wave function for the overtone was derived in a first-order perturbation approach using a harmonic oscillator basis and by developing the potential up to cubic terms. Deleting from the first-order function the term in the resonance denominator $\omega - 2\omega_4$ resulted in our approximation to the wave function for the Fermi-unperturbed overtone. This approximate function was subsequently used to calculate the corresponding transition dipole. For this, the dipole moment was expanded to second order. For the C_s complexes the additional approximation was made that the second-order derivatives with respect to X_4 and Y_4 are identical.

We used the literature data for the cubic coupling constants,³⁴ $\alpha_{244} = -6.3 \text{ cm}^{-1}$ and $\alpha_{344} = 6.8 \text{ cm}^{-1}$, and for the dipole moment derivatives,²⁷ $(\partial \mu_z / \partial Q_2)_e = 0.23 \text{ D}$ and $(\partial \mu_z / \partial Q_3)_e = 0.12 \text{ D}$, for monomer Fl. They were assumed to be unaltered by the complexation. The coupling constant α_{144} and dipole moment derivatives with respect to Q_1 and $(X_4^2 + Y_4^2)$ were calculated numerically, by using a polynomial expansion in terms of two pairs of dimensionless normal coordinates $[Q_1, X_4]$ and $[X_4, Y_4]$ in the region $[-2, -1, 0, 1, 2]$ for monomer Fl and for the complex Fl·Am, at the MP2/6-31+G(d,p) level. As an example, the values for these parameters for monomer Fl and for the complex with Am are shown in Table 4 together with the unperturbed transition dipole moments for the overtone level.

The Fermi resonance mixes the vibrational states, and the transition moments for the high frequency (hf) and low frequency (lf) perturbed states can be written as

$$\langle \mu_z \rangle_{\text{hf}} = a \langle 00 | \mu_z | 10 \rangle + b \langle 00 | \mu_z | 02^0 \rangle^0 \quad (7a)$$

$$\langle \mu_z \rangle_{\text{lf}} = -b \langle 00 | \mu_z | 10 \rangle + a \langle 00 | \mu_z | 02^0 \rangle^0 \quad (7b)$$

where

$$a = \sqrt{\frac{\kappa + \Delta}{2\kappa}}, \quad b = \frac{W}{|W|} \sqrt{\frac{\kappa - \Delta}{2\kappa}} \quad (8)$$

Combining eqs 7 and 8, it is straightforward to show that the intensity ratio of the Fermi doublet is

$$R = \frac{\kappa + \Delta}{\kappa - \Delta} \left(\frac{1 + \frac{4W}{(\kappa + \Delta)\sqrt{R_0}} + \frac{(\kappa - \Delta)}{(\kappa + \Delta)R_0}}{1 - \frac{(\kappa + \Delta)}{W\sqrt{R_0}} + \frac{(\kappa + \Delta)}{(\kappa - \Delta)R_0}} \right) \quad (9)$$

where

$$\sqrt{R_0} = \langle 00 | \mu_z | 10 \rangle / \langle 00 | \mu_z | 02^0 \rangle^0 \quad (10)$$

The calculation of R as a function of α_{144} requires a value for R_0 . The results in Table 4 show that our calculations lead to

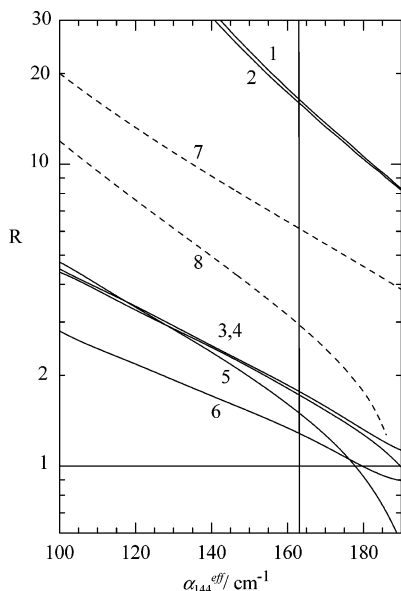


Figure 4. Calculated values for the relative intensity R as a function of the cubic coupling constant $\alpha_{144}^{\text{eff}}$: (1) FI in LXe, 188 K; (2) FI in LAr, 90 K; (3) FI·Am in LXe, 188 K; (4) FI·Py in LXe, 188 K; (5) FI·TMA in LAr, 90 K; (6) FI·DME in LAr, 90 K; (7) FI in LAr, 90 K, zero-intensity approximation; (8) FI·TMA in LAr, 90 K, zero-intensity approximation.

second-order transition moments for FI and for FI·Am that are very nearly the same. We have extrapolated this conclusion, so that for all complexes the same value of 0.006 D could be used. For the first-order transition moment in the nominator of R_0 the experimental values in Table 2 were used.

It can be seen from Table 4 that the anharmonic characteristics, α_{144} and the dipole second derivative, are hardly affected by the complexation. In contrast, the harmonic characteristic, $(\partial\mu_z/\partial Q_1)_e$ changes significantly, having a negative value in the monomer but a positive one in the complex. This is the main contribution to the sharp change in the intensity ratio R upon complexation.

Values of R as function of $\alpha_{144}^{\text{eff}}$ are shown in Figure 4. Values of R obtained for the optimized value of $\alpha_{144}^{\text{eff}} = 163 \text{ cm}^{-1}$ are given in Table 2. Taking into account the various approximations in the model used, and accounting for the problems encountered in deriving the experimental values, which is obvious from the spectra in Figure 1, the results in Table 2 show that our approach leads to a satisfactory reproduction of the sharp change in the value of R upon complexation.

Although the practice was discouraged a long time ago,³⁶ for reasons of simplification some authors make the assumption that the infrared intensity of the unperturbed overtone of a Fermi doublet can be neglected. It is of interest to see where this is leading to for the present case. For $\sqrt{R_0} = 0$, expression 9 reduces to $R = (\kappa + \Delta)/(\kappa - \Delta)$. Thus, in this approximation R is given as a function of the experimentally measured quantity κ , and of Δ . The accuracy of the latter is judged high because it is derived from κ and from the well-defined value of α_{144} determined in this study. Hence, if the zero-intensity approximation is valid, the R values calculated with it should agree better with the observed ones than those calculated with relation 6, in which less reliable quantities have been used to derive R_0 . Figure 4 contains the R curves obtained for this model, for monomer FI in trace 7, and for FI·TMA in trace 8. It can be seen that this approximation leads to a poor result, R changing from monomer to complex by not more than a factor of 2.5. This is significantly further away from the experimentally observed change than the

change obtained for the nonzero intensity model. This, evidently, supports previous conclusions on the poor performance of the zero-intensity overtone model.³⁶

Conclusions

In this study, some new experimental data on the complexes of fluoroform with ammonia and pyridine are presented. The complexation is found to induce blue shifts in ν_1 of fluoroform. At the same time significant increases are observed in the intensity of $2\nu_4$ of the Lewis acid, signaling changes in the Fermi resonance between ν_1 and $2\nu_4$. Our subsequent analysis shows that the Fermi-corrected value of ν_1 in the pyridine complex is in fact red shifted from the monomer value, while for the ammonia complex the corrections reduce the shift to a value below the threshold that allows the type of interaction to be identified. We, therefore, propose to designate the observed shifts in these complexes as pseudo-blue shifts.

Fermi-corrected ν_1 values in the complexes of fluoroform with dimethyl ether and trimethyl amine were obtained similarly. For the dimethyl ether complex, for which ν_1 is blue shifted considerably, the Fermi correction has little influence on the ν_1 frequency and does not change its sign. For the trimethyl amine complex, for which a significant red-shift is observed, the correction for Fermi resonance substantially increases the shift, and, evidently, also does not change its sign.

As a general conclusion it may be stated that in order to correctly interpret complexation shifts of the C–H stretch of fluoroform it is required to correct the observed frequencies for the Fermi resonance of this mode with $2\nu_4$.

Acknowledgment. The authors thank Dr. P. Rodziewicz for helpful discussions. The authors thank the FWO-Vlaanderen for its assistance toward the purchase of the spectroscopic equipment used in this study and for a research grant toward one of us (S.N.D.). Financial support from the Flemisch Community and the University of Antwerp, through the Special Research Fund (BOF) and the RAFO Research Grants is also acknowledged. D.N.S., S.M.M., and K.S.R. acknowledge support from RFBR (Grant No. 05-03-33235a).

References and Notes

- (1) Hussein, M. A.; Millen, D. J. *J. Chem. Soc. Faraday Trans.* **1976**, *72*, 693.
- (2) Bertsev, V. V.; Golubev, N. S.; Shchepkin, D. N. *Opt. Spektrosk.* **1976**, *40*, 951.
- (3) Golubev, N. S.; Kolomitsova, T. D.; Melikova, S. M.; Shchepkin, D. N. *Teor. Spektrosk., Izv. Akad. Nauk. SSSR (in Russian)* **1977**, *78*.
- (4) Paulson, S. L.; Barnes, A. J. *J. Mol. Struct.* **1982**, *80*, 151.
- (5) Fraser, G. T.; Lovas, F. J.; Suenram, R. D.; Nelson, D. D.; Klempner, W. *J. Chem. Phys.* **1986**, *84*, 5983.
- (6) Gu, Y. L.; Kar, T.; Scheiner, S. *J. Am. Chem. Soc.* **1999**, *121*, 9411.
- (7) Hobza, P.; Havlas, Z. *Chem. Rev.* **2000**, *100*, 4253.
- (8) Scheiner, S.; Grabowski, S. J.; Kar, T. *J. Phys. Chem. A* **2001**, *105*, 10607.
- (9) Van der Veken, B. J.; Herrebout, W. A.; Szostak, R.; Shchepkin, D. N.; Havlas, Z.; Hobza, P. *J. Am. Chem. Soc.* **2001**, *123*, 12290.
- (10) Delanoye, S. N.; Herrebout, W. A.; Van der Veken, B. J. *J. Am. Chem. Soc.* **2002**, *124*, 11854.
- (11) Delanoye, S. N.; Herrebout, W. A.; Van der Veken, B. J. *J. Am. Chem. Soc.* **2002**, *124*, 7490.
- (12) Hobza, P.; Havlas, Z. *Theor. Chem. Acc.* **2002**, *108*, 325.
- (13) Kryachko, E. S.; Zeegers-Huyskens, T. *J. Mol. Struct.* **2002**, *615*, 251.
- (14) Li, X. S.; Liu, L.; Schlegel, H. B. *J. Am. Chem. Soc.* **2002**, *124*, 9639.
- (15) Melikova, S. M.; Rutkowski, K. S.; Rodziewicz, P.; Koll, A. *Pol. J. Chem.* **2002**, *76*, 1271.
- (16) Melikova, S. M.; Rutkowski, K. S.; Rodziewicz, P.; Koll, A. *Chem. Phys. Lett.* **2002**, *352*, 301.
- (17) Scheiner, S.; Kar, T. *J. Phys. Chem. A* **2002**, *106*, 1784.

- (18) Zierkiewicz, W.; Michalska, D.; Havlas, Z.; Hobza, P. *ChemPhys-Chem* **2002**, *3*, 511.
- (19) Hermansson, K. *J. Phys. Chem. A* **2002**, *106*, 4695.
- (20) Karpfen, A.; Kryachko, E. S. *J. Phys. Chem. A* **2003**, *107*, 9724.
- (21) Pejov, L.; Hermansson, K. *J. Chem. Phys.* **2003**, *119*, 313.
- (22) Kryachko, E.; Scheiner, S. *J. Phys. Chem. A* **2004**, *108*, 2527.
- (23) Rhee, S. K.; Kim, S. H.; Lee, S.; Lee, J. Y. *Chem. Phys.* **2004**, *297*, 21.
- (24) Van den Kerkhof, T.; Bouwen, A.; Goovaerts, E.; Herrebout, W. A.; Van der Veken, B. J. *J. Phys. Chem. Chem. Phys.* **2004**, *6*, 358.
- (25) Simon, S.; Duran, M.; Dannenberg, J. J. *J. Chem. Phys.* **1996**, *105*, 11024.
- (26) Frisch, M. J.; Trucks, G. W.; Schlegel, H. B.; Scuseria, G. E.; Robb, M. A.; Cheeseman, J. R.; Montgomery, J. A., Jr.; Vreven, T.; Kudin, K. N.; Burant, J. C.; Millam, J. M.; Iyengar, S. S.; Tomasi, J.; Barone, V.; Mennucci, B.; Cossi, M.; Scalmani, G.; Rega, N.; Petersson, G. A.; Nakatsuji, H.; Hada, M.; Ehara, M.; Toyota, K.; Fukuda, R.; Hasegawa, J.; Ishida, M.; Nakajima, T.; Honda, Y.; Kitao, O.; Nakai, H.; Klene, M.; Li, X.; Knox, J. E.; Hratchian, H. P.; Cross, J. B.; Adamo, C.; Jaramillo, J.; Gomperts, R.; Stratmann, R. E.; Yazyev, O.; Austin, A. J.; Cammi, R.; Pomelli, C.; Ochterski, J. W.; Ayala, P. Y.; Morokuma, K.; Voth, G. A.; Salvador, P.; Dannenberg, J. J.; Zakrzewski, V. G.; Dapprich, S.; Daniels, A. D.; Strain, M. C.; Farkas, O.; Malick, D. K.; Rabuck, A. D.; Raghavachari, K.; Foresman, J. B.; Ortiz, J. V.; Cui, Q.; Baboul, A. G.; Clifford, S.; Cioslowski, J.; Stefanov, B. B.; Liu, G.; Liashenko, A.; Piskorz, P.; Komaromi, I.; Martin, R. L.; Fox, D. J.; Keith, T.; Al-Laham, M. A.; Peng, C. Y.; Nanayakkara, A.; Challacombe, M.; Gill, P. M. W.; Johnson, B.; Chen, W.; Wong, M. W.; Gonzalez, C.; Pople, J. A. Gaussian03; Revision A.5 ed.; Gaussian, Inc.: Pittsburgh, PA, 2003.
- (27) Kondo, S.; Saeki, S. *J. Chem. Phys.* **1981**, *74*, 6603.
- (28) Dubal, H. R.; Quack, M. *J. Chem. Phys.* **1984**, *81*, 3779.
- (29) Dubal, H. R.; Ha, T. K.; Lewerenz, M.; Quack, M. *J. Chem. Phys.* **1989**, *91*, 6698.
- (30) Fyke, N. J.; Lockett, P.; Thompson, J. K.; Wilt, P. M. *J. Mol. Spectrosc.* **1975**, *58*, 87.
- (31) Borgest, V. A.; Kolomiitsova, T. D.; Shchepkin, D. N. *Opt. Spektrosk.* **1976**, *40*, 63.
- (32) Green, W. H.; Lawrance, W. D.; Moore, C. B. *J. Chem. Phys.* **1987**, *86*, 6000.
- (33) Amos, R. D.; Gaw, J. F.; Handy, N. C.; Carter, S. *J. Chem. Soc. Faraday Trans.* **1988**, *84*, 1247.
- (34) Klatt, G.; Willetts, A.; Handy, N. C.; Tarroni, R.; Palmieri, P. *J. Mol. Spectrosc.* **1996**, *176*, 64.
- (35) Melikova, S. M.; Herrebout, W. A.; Rutkowski, K. S.; Shchepkin, D. N.; Maholl, S.; van der Veken, B. J., to be published.
- (36) McKean, D. C. *Spectrochim. Acta A* **1973**, *A 29*, 1559.